行政院國家科學委員會專題研究計畫　成果報告

極高能宇宙射線之能量測量

計畫類別：個別型計畫
計畫編號：NSC94-2112-M-009-026-
執行期間：94 年 08 月 01 日至 95 年 07 月 31 日
執行單位：國立交通大學物理研究所

計畫主持人：林貴林

計畫參與人員：張鳳吟、劉宗哲、張鑑源、董念恩

報告類型：精簡報告
報告附件：出席國際會議研究心得報告及發表論文
處理方式：本計畫可公開查詢

中　華　民　國 95 年 10 月 31 日

一、中文摘要

本篇報告從 28.5 GeV 電子束引發不同深度電磁簇射所產生大氣螢光的測量，得到的光效益將和簇射中離子化截面的預測與觀察結果作比較，以證實使用大氣螢光截面測量極高能宇宙射線的正當性。同時本篇也報告利用同步輻射中心 1.5 GeV 電子束研究大氣螢光的性質，我們利用閃爍器來測量簇射的橫截面，並更進一步發掘使用同步輻射器材來測量簇射中切倫科夫輻射的可能性。

關鍵詞：螢光，簇射

Abstract

Measurements are reported on the fluorescence of air as a function of depth in electromagnetic showers initiated by bunches of 28.5 GeV electrons. The light yield is compared with the expected and observed depth profiles of ionization in the showers. It validates the use of atmospheric fluorescence profiles in measuring ultra high energy cosmic rays.

An effort of using NSRRC 1.5 GeV electron beam for studying air shower properties is reported. The shower lateral profile is measured by the scintillator technique. Furthermore we explore the possibility of measuring the shower Cherenkov radiation with the NSRRC facility.

Keywords: Fluorescence, Showers

二、緣由與目的

The cosmic ray spectrum above 10^{19} eV is not yet well understood [1]. Mechanisms leading to such high energies have been proposed, either by acceleration from very energetic sources [2] or by decays of primordial super heavy particles [3]. However, neither scenario are supported by strong evidences. In the experimental aspect, the spectrum reported by the AGASA detector [4], an array of scintillators covering 100 km^2 at ground level, is both more intense and extends to higher energy than that of the atmospheric fluorescence detector, HiRes [5]. We note that the former result seems to violate the cutoff in the ultrahigh energy cosmic ray (UHECR) spectrum, which is expected from the interactions between UHECR and the cosmic microwave background radiation known as the GZK effect [6]. Therefore further experiments are needed to clarify the situation, and to enhance the presently very limited statistics. There are several experiments under considerations, in planning or under construction [7]. All of these include at least a fluorescence measurement system for atmospheric showers.

The successes of the above fluorescence technique require energy calibrations of the detectors. To perform such energy calibrations, it is important to realize that the electron-positron spectrum is maintained similar in shape in all showers, independent of initial energy, aside from the relatively sparsely populated high energy tail [8]. The spectrum is principally dependent on the shower age, $S=3X/(X+2X_{max})$ where X is the depth into the shower, and X_{max} the depth at shower maximum [9]. Therefore UHECR showers may be viewed as a vast superposition of showers re-initiated by electrons and gamma rays of a wide range of low energies. Studies of showers initiated by accelerator beams are immediately applicable to them. This observation leads to the

FLASH experiment which can calibrate the fluorescence measurement using SLAC 28.5 GeV electron beam. Such calibrations intend to answer two important questions: how well do we know the fluorescence efficiency and can the fluorescence yield accurately reconstruct the shower longitudinal profile? The first issue is tackled in the FLASH thin target run experiment [10]. Specifically the absolute yield of light in the relevant wavelength band, and its spectrum, as a function of atmospheric pressure is studied in this run.

In this report, I shall focus on the second issue, which is studied in the FLASH thick target experiment [11]. The technique of this experiment will be also applied in the experiment using NSRRC 1.5 GeV electron beam. The air shower is simulated by injecting SLAC 28.5 GeV electron beam on the target bricks made of Al_2O_3 with 10 % SiO_2. The measured mean density of the bricks was 3.51 g cm^{-3}. The radiation length, 28 g cm^{-2}, is just 24% less than that of air, and the critical energy, below which ionization energy loss dominates, is 54 MeV, compared with 87 MeV for air. A schematic view of the apparatus can be found in [11]. The alumina was contained in a line of four aluminum boxes that could remotely and independently be moved on or off the beam line. The downstream block was approximately 2 radiation lengths (15 cm) thick, by 50 cm wide, and the air fluorescence detector was placed immediately behind it. Each of the upstream blocks was 4 radiation lengths thick. This arrangement permitted thicknesses of approximately 0, 2, 6, 10 and 14 radiation lengths to be selected, with negligible gaps, immediately in front of the detector. In this way the longitudinal profile of an electromagnetic shower could be developed. In addition, thickness of 4, 8 and 12 radiation lengths could be studied, but in this case there was a 15 cm air gap in front of the detector, and the downstream alumina block, which could only be extracted 6 cm beyond the beam line, partially occluded the shower tail. The shower particles leaving the alumina immediately entered the detector volume, where they caused a flash of fluorescence in the layer of air at atmospheric pressure. The detector was in the form of a flat rectangular aluminum box, its air space 6 cm thick along the beam direction, and with vertical dimension, 50 cm, matching the alumina. Some of the light traveled towards a vertical row of photomultiplier tubes mounted on one side. It was necessary to take steps to suppress the accidental collection of the forward going Cherenkov light from the air as well as fluorescence light scattered from the walls. The suppression was done in the standard way, using a set of 1 cm wide vertical baffles on the front and back walls, and all surfaces, except mirrors and photomultiplier tube (PMT) apertures, were covered with black flock material [12]. Behind the air fluorescence chamber there was space for measuring other aspects of the showers. Taiwan team was responsible for measuring shower's lateral profile using a standard beam scintillation screen. By means of mirrors, the light was imaged by a CCD camera in a heavily shielded enclosure, and data collected by a remote screen-capture system. In the same space, a flat plate ion chamber was installed to measure the shower longitudinal charge profile. The ion chamber was designed for the high radiation and ionization levels, and wide dynamic range, encountered after the shower media. It used 11 active gaps, nominally 0.9 mm thick, with plates based on printed circuit board covering the 50 cm square active width of the air fluorescence chamber. The gas was helium at 1 atmosphere, and the applied voltage, 140 V/mm, was chosen to maximize the clearing field and electrode charge without leading to gas gain. All anodes were connected electrically, as were all cathodes. Their signals were read out without amplification.

Concerning our works with NSRRC electron beam, it is interesting to explore the possibility of simultaneously studying shower longitudinal and lateral profiles. Such studies are carried out with Taiwan's NSRRC 1.5 GeV electron beam [13]. Although the beam energy is only 1.5 GeV, the beam current is large enough to produce a total energy of the order 0.1 to 1 EeV. We perform the shower profile measurement by shooting the NSRRC 1.5 GeV electron beams on aluminum targets. The shower parameters of aluminum are comparable to those of alumina used in the FLASH experiment. The radiation length of aluminum is 24.01 g/cm^2 compared to 27.94 g/cm^2 of Al_2O_3 while the radiation length of aluminum is 52.55 MeV compared to 54 MeV of Al_2O_3. A scintillator (Al_2O_3: Cr) is placed behind the targets, converting the secondary shower particles into light. The light from the central region of the shower is recorded by a CCD camera while the light from the outer region is monitored by PMTs.

The CCD system is successfully implemented in the FLASH thick target run as just mentioned.

The instrument is a platform of two chambers and a removable aluminum blocks system which contains 15 aluminum blocks. Each block can be moved in or out of the beam path. Therefore, it is possible to study shower longitudinal profile in 15 steps, with an increment of 1/3 radiation length (R.L.) per step. The top view of the experimental platform can be found in Ref. [13]. Left chamber contains a 6-hole wheel which can accommodate several different materials or calibration light sources for the experiment. One can perform the spectrometer experiment by placing the scintillator in the wheel, to be hit by the electron beam, and measuring the light outside the chamber. The central part of the platform consists of 15 movable aluminum blocks. The size of each block is 10 cm×10 cm×2.9 cm. Finally, the right chamber is for measuring the lateral profile. Electron beams enter into the left chamber and produce showers in the aluminum blocks. The resulting secondary charge particles travel through the right chamber and hit the scintillator screen. The light reflected from the scintillator is subsequently detected. Because of the large dynamic range of the electron density in the lateral profile, two types of detectors are used. A CCD camera takes the image in the high electron density region, while a PMT system works for the low electron density region.

Scintillator (AF995r ; Al_2O_3 :Cr^{3+}) is widely used for monitoring the beam. It is a material with high damage threshold, and high photon yield. Ref. [14] shows a spectrum of fluorescence photons with only one decay time 3.4 ms listed. To accurately reconstruct the shower lateral profile from the scintillation light, we first measure the wavelength and decay time of the scintillator spectrum. Since the electron beam is injected from booster ring with a 10 Hz frequency, it is necessary to measure the decay time of the scintillation light in order to access the influence of scintillation light from a certain event to the signal of subsequent events. We will show in the next session a decay time measurement using a photo-diode and digital multi-meter.

The Cherenkov radiation is an important background to the fluorescence light measurement. The Cherenkov radiation from each individual charge particle is well known. Hence the uncertainty on the Cherenkov radiation in an air shower is due to the uncertainty in energy distributions of shower particles. It is well known that an electron with energy less than 100 MeV emits appreciable less numbers of Cherenkov photons than the saturated value. For calculating Cherenkov radiation in air showers, the parameterization by Hillas [15] for electron energy distributions at a fixed shower age has been widely used. Such an energy distribution is obtained from air showers induced by a primary 100 GeV primary photon. However, a recent study using

CORSIKA [16] and QGSJET01 [17] simulations gives a different parameterization for electron energy distributions and subsequently the resulting Cherenkov radiations [18]. The electron energy distributions in terms of the shower age are found to be universal, i.e., independent of the type and energy of the primary particle. This new electron energy distribution could result into a Cherenkov radiation deviating from that given by Hillas' parameterization by as much as 20% depending on the viewing angle to the shower axis [19]. Since the accuracy of fluorescence measurement depends on a correct subtraction of Cherenkov contamination, it is important to directly measure such a contribution.

We are investigating the possibility of measuring Cherenkov radiation from air showers using the NSRRC 1.5 GeV electron beam. Geant4 [20] simulations of charge particle longitudinal profile and Cherenkov photon yield will be presented in the next session.

三、結果與討論

Both results of fluorescence and ion chamber measurements are presented in the Fig. 1 [11], where the light profile (the average of the three PMTs), and the ion chamber profile measured at a slightly different shower depth, are independently normalized to sum to unity. The agreement between two profiles demonstrate the proportionality of charge particle number and the resulting fluorescence yield, an assumption in the fluorescence technique for measuring the energy of primary cosmic ray particles.

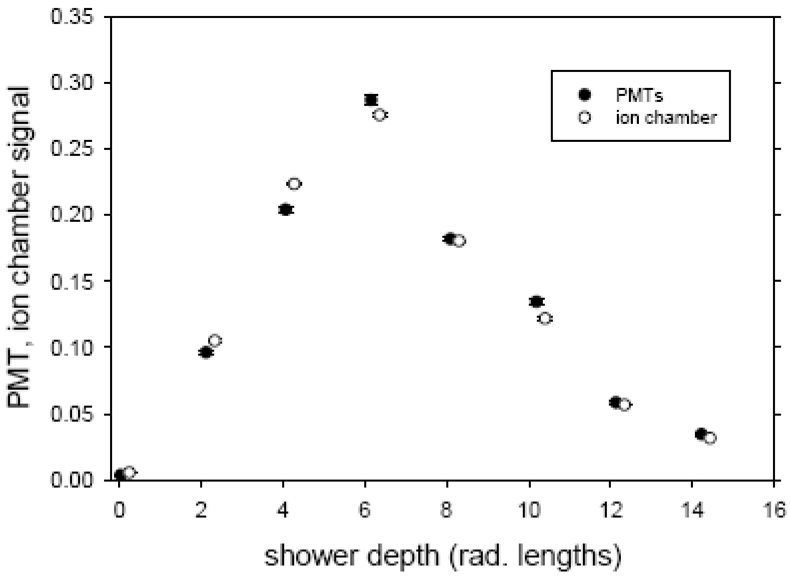

Fig. 1 Comparison of fluorescence and ionization longitudinal profiles. The sums of their points are independently normalized to unity.

In additional to the shower longitudinal profile, we also obtain results for the lateral spreads of the showers as depicted in Fig. 2 [11]. The figure compares the results of the EGS4 model with a profile from the scintillation screen and camera. The agreement in the transverse distribution, although not perfect, is quite satisfactory for our purposes. The transverse containment of the showers by the fluorescence and ion chambers was evidently well modeled by the simulations. Even at this depth in the shower, the characteristic sharp central peak remains. It is this peak that gives rise to the small non-linear effects in the ion chamber.

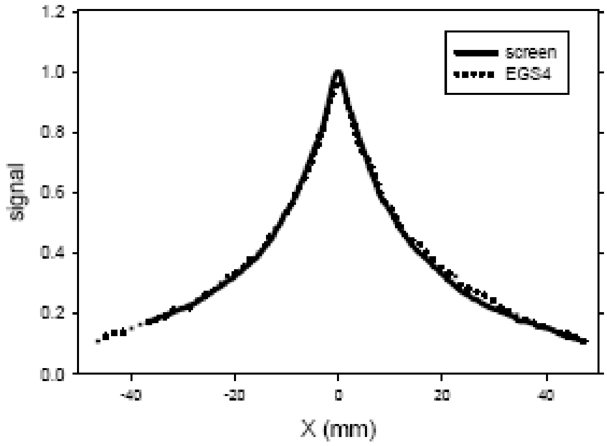

Fig. 2 Shower spread at 10 radiation lengths, projected on to x-axis. Y-axis range is ± 4.8 cm

Concerning the NSRRC project, we have mentioned earlier the necessity of measuring the decay spectrum of scintillator. Fig. 3 shows results of such a measurement.

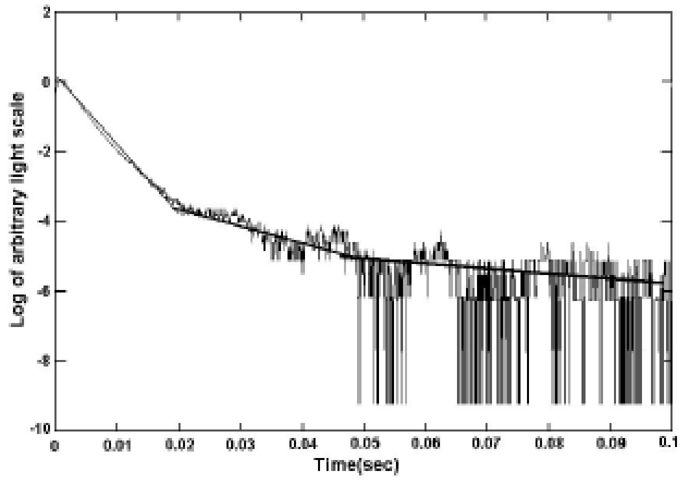

Fig. 3 Results from the decay-time measurement. This decay-time of the scintillation light from ($Al_2O_3:Cr^{3+}$) is measured by photo-diode and digital multi-meter. The first decay pattern has a decay time of 3.4 ms, the second one has a decay time of 6.7 ms and the third one has a decay time longer than 15 minutes.

Photons produced by scintillator ($Al_2O_3:Cr^{3+}$) are detected by a photo-diode. Their signals show a rise in the first few ms, believed to be the electronic response time. It is then followed by several exponential decays. At least three distinct decay patterns are observed. The first one has a decay time of 3.4 ms, the second one has a decay time of 6.7 ms and the third one has a decay time longer than 15 minutes. Fig. 4 shows the fluorescence spectrum of the scintillator. The spectrum show two close peaks located at wavelengths 694.0 nm and 692.8 nm respectively.

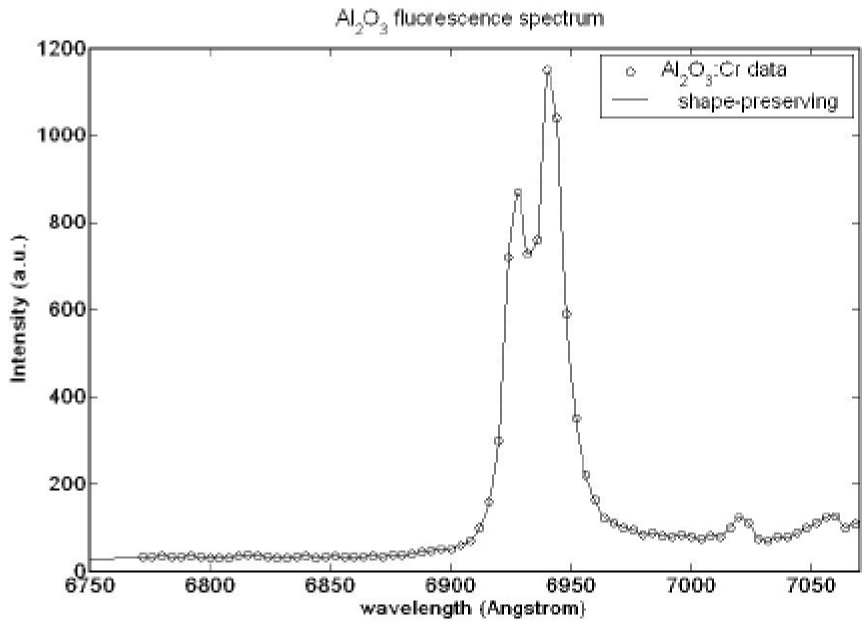

Fig. 4 The fluorescence spectrum of $Al_2O_3:Cr^{3+}$ scintillator. Two close peaks located at wavelengths 692.8 nm and 694.0 nm are clearly seen.

The measurements of $Al_2O_3:Cr^{3+}$ fluorescence spectrum and the corresponding decay times are performed with a narrow band filter allowing radiations of the wavelength range (694.3± 5) nm. Such a band width is however still too large to isolate each peak in the spectrum and study its individual decay properties. We obtain the shower longitudinal profile as shown in Fig. 5.

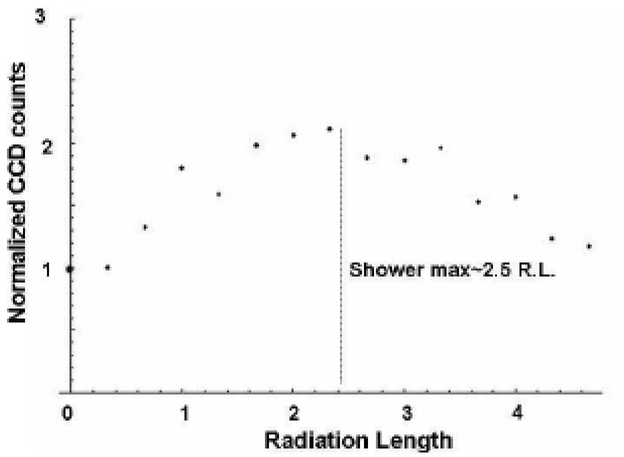

Fig. 5 The shower longitudinal profile as recorded by the CCD camera.

The shower maximum is seen to occur at 2.5 radiation length, rather than 2.3 radiation length obtained from simulations. Furthermore the normalized CCD counts do not behave like a smooth function. These two behaviors of the data are due to effects of the slowest decay component, namely the component with a decay time more than 15 minutes, of the fluorescence spectrum. In particular, since the fluorescence light from the earlier events can contribute to signals of later events, the peak of the longitudinal profile recorded by CCD camera is then shifted from the anticipated 2.3 radiation length. Clearly, to remove the effect of slowest decay component, a more careful study on the decay time of $Al_2O_3:Cr^{3+}$ down to each fluorescence peak is necessary.

Concerning the measurement of Cherenkov radiation from air showers, the Geant4 [20] simulations of charge particle longitudinal profile and Cherenkov photon yield are presented in Fig. 6, where we have set the charge particle energy threshold at 1 MeV.

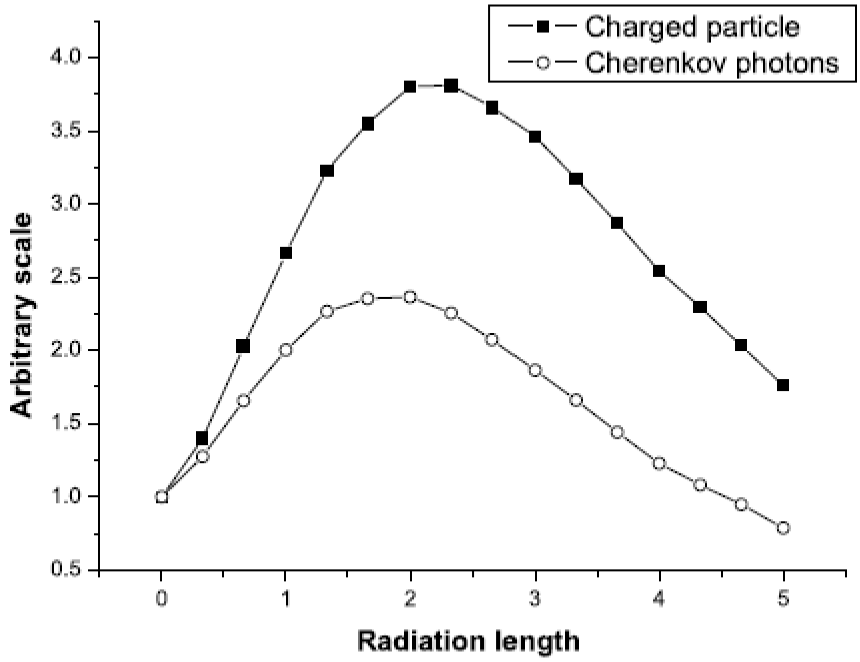

Fig. 6 The longitudinal profile and Cherenkov photon yield as a function of radiation length.

At the zero radiation length, the energy of each charge particle is 1.5 GeV. Since this energy is well beyond the 22 MeV threshold, the number of Cherenkov photons emitted by each charge particle already reaches the maximum value. We then choose to normalize two curves (longitudinal profile and Cherenkov photon yield) at zero radiation length. The two curves begin to deviate for higher radiation lengths. At the shower maximum, i.e., 2.3 radiation length, the Cherenkov photon yield drops to 60% of the maximum value. This is due to the increase of low energy charge particle which either can not produce Cherenkov photon or produces appreciable less number of Cherenkov photons than the maximum value. It is clear that different electron energy distributions are reflected in the different Cherenkov photon yield. Detail simulations of Cherenkov photon measurement are in progress.

四、計畫成果自評

The FLASH experiments are successfully performed and data analyses are completed. The thin target test run was published [10]. The thick target paper has also been published [11]. The result of thick target run validates the use of atmospheric fluorescence profiles in measuring the energy of ultrahigh energy cosmic ray particle. This is important in view of the discrepancy between fluorescence based HiRes experiment and the ground array based AGASA experiment. The detailed analysis on the efficiency of each individual fluorescence line shall have important impacts on the Pierre Auger experiment. This part of work will be finished by the end of 2006 [21].

Concerning the local effort at NSRRC, we have simultaneously measured the shower longitudinal and lateral profiles using scintillator screen and CCD camera. We have found that it is necessary to isolate each spectrum peak of $Al_2O_3:Cr^{3+}$ scintillator screen so that the slowest-decay component of fluorescence spectrum can be identified. With a suitable filter, this slowest-decay component may be removed. The less satisfactory result on the shower profile measurement prompted us to explore the possibility of measuring Cherenkov radiation from air showers using the same NSRRC electron beam. Currently we not only perform the simulation studies but also acquire some data of Cherenkov radiation from particle showers. The data analysis is in progress.

In addition to FLASH and NSRRC experiment, we also completed a work on the neutrino physics. This work discusses the strategy of probing θ_{23} octant in the very long baseline neutrino oscillation experiments, including future atmospheric neutrino experiments. We have identified the optimal baselines and neutrino energies for this purpose [22].

五、參考文獻

[1] G. Sigl, Ann. Phys. 303, 117 (2003).

[2] E. Waxman, Phys. Rev. Lett. 75, 386 (1995); M. Vietri, Astrophys. J. 453, 883 (1995); T.K. Gaiser, F. Halzen and T. Stanev, Phys. Rep. 258, 173 (1995); K. Mannheim, Astropart. Phys. 3, 295 (1995).

[3] M. Birkel and S. Sarkar, Astropart. Phys 9, 297 (1998); P. Battacharjee, C.T. Hill and D.N. Schramm, Phys. Rev. Lett. 69, 567 (1992); R.J. Protheroe and T. Stanev, Phys. Rev. Lett. 77, 3708 (1996); M. Birkel and S. Sarkar, Astropart. Phys. 9, 297 (1998); P. Battacharjee and G. Sigl, Phys. Rep. 327, 109 (2000).

[4] M. Takeda et al., Astrophys. J. 522, 225 (1999).

[5] R. Abbasi et al., Phys. Rev. Lett. 92, 151101 (2004).

[6] K. Greisen, Phys. Rev. Lett. 16, 748 (1966); V.A. Kuzmin, G.T. Zatsepin, Pisma Zh. Eksp. Teor. Fiz. 4, 114 (1966).

[7] J. Abraham et al., Nucl. Instr. Meth. A 523, 50 (2004); M. Fukushima, Institute for Cosmic Ray Research Mid-Term (2004-2009) Maintenance Plan Proposal Book ``Cosmic Ray Telescope Project", Tokyo Univ., (2002); L. Scarsi et al., Proc. 27th International Cosmic Ray Conf., Copernicus Gesellschaft, Hamburg, 175, (2002); J, Linsley, Proc., 26th International Cosmic Ray Conf., Univ. Utah, Salt Lake City Vol. 2, 423 (1999).

[8] M. Risse and D. Heck, Astropart. Phys. 20, 661 (2004); F. Nerling et al., Proc. 28th International Cosmic Ray Conf., Universal Academy Press 2003, p. 611; C. Song et al., Astropart. Phys 14, 7 (2000).

[9] A. Hillas, J. Phys. G 8, 1461 (1982).

[10] J. Belz et al. [FLASH collaboration], SLAC Experimental Proposal E-165 (2002); J. Belz et al. [FLASH collaboration], Astropart. Phys. 25, 129 (2006).

[11] Belz et al., Astropart. Phys. 25, 57 (2006).

[12] Edmund Optics, Barrington, NJ08007 U.S.A., www.edmundoptics.com.

[13] T. C. Liu, F. Y. Chang, C. C. Chen, C. W. Chen, M. A. Huang, W.-Y. P. Hwang, and G. L. Lin, Proc., 29th International Cosmic Ray Conf., Pune, India, Aug. 3-10, 2005,tai-liu-TC-abs1-he15-oral.pdf.

[14] K.J. McCarthy, et al., J. of Applied Phys. 92, 6541 (2002).

[15] A. M. Hillas, J. Phys. G 8, 1461 (1982).

[16] D. Heck et al., Report FZKA 6019 (Forschungszentrum Karlsruhe) (1998).

[17] N. N. Kalmykov, S. S. Ostapchenko, A. I. Pavlov, Nucl. Phys. B (Proc. Suppl.) 52,

17 (1997).
[18] F. Nerling et al., Astropart. Phys. 24, 321 (2006).
[19] F. Nerling et al., astro-ph/0507251.
[20] Geant4 Collaboration, S. Agostinelli et al., Nucl. Instr. And Meth. A 506, 250 (2003).
[21] J. Belz et al. [FLASH collaboration], paper in preparation.
[22] G.-L. Lin and Y. Umeda, to be submitted.